Biomedicine & Pharmacotherapy 168 (2023) 115791

Contents lists available at ScienceDirect

Biomedicine & Pharmacotherapy

journal homepage: www.elsevier.com/locate/biopha

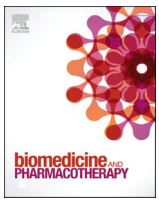

Discovery of a synthetic taiwaniaquinoid with potent *in vitro* and *in vivo* antitumor activity against breast cancer cells

Nuria Mut-Salud [a], Juan J. Guardia [b], Antonio Fernández [b], Isabel Blancas [a,c,d,e], Houda Zentar [b], José M. Garrido [a,e,f], Enrique Álvarez-Manzaneda [b], Rachid Chahboun [b,*], Fernando Rodríguez-Serrano [a,e,g,**]

[a] *Biopathology and Regenerative Medicine Institute (IBIMER), University of Granada, Granada 18016, Spain*
[b] *Department of Organic Chemistry, Faculty of Sciences, University of Granada, Granada 18071, Spain*
[c] *Department of Medicine, School of Medicine, University of Granada, Granada 18016, Spain*
[d] *Department of Medical Oncology, San Cecilio University Hospital, Granada 18016, Spain*
[e] *Biosanitary Research Institute of Granada (ibs.GRANADA), Granada 18014, Spain*
[f] *Department of Surgery and Surgical Specialties, University of Granada, Granada 18016, Spain*
[g] *Department of Human Anatomy and Embryology, Faculty of Medicine, University of Granada, Granada 18016, Spain*

ARTICLE INFO

Keywords:
Taiwaniaquinoids
Cancer
Apoptosis
Cell cycle arrest
Oxidative stress
In vivo

ABSTRACT

Taiwaniaquinoids are a unique family of diterpenoids predominantly isolated from Taiwania cryptomerioides Hayata. Previously, we evaluated the antiproliferative effect of several synthetic taiwaniaquinoids against human lung (A-549), colon (T-84), and breast (MCF-7) tumor cell lines. Herein, we report the *in vitro* and *in vivo* antitumor activity of the most potent compounds. Their cytotoxic activity against healthy peripheral blood mononuclear cells (PBMCs) has also been examined. We underscore the limited toxicity of compound **C36** in PBMCs and demonstrate that it exerts its antitumor effect in MCF-7 cells ($IC_{50} = 1.8$ μM) by triggering an increase in reactive oxygen species, increasing the cell population in the sub-G_1 phase of the cell cycle (90 %), and ultimately activating apoptotic (49.6 %) rather than autophagic processes. Western blot results suggested that the underlying mechanism of the **C36** apoptotic effects was linked to caspase 9 activation and a rise in the Bax/Bcl-2 ratio. *In vivo* analyses showed normal behavior and hematological parameters in C57BL/6 mice post **C36** treatment. Moreover, no significant impact was observed on the biochemical parameters of these animals, indicating that **C36** did not induce liver toxicity. Furthermore, **C36** demonstrated a significant reduction in tumor growth in immune-competent C57BL/6 mice implanted with E0771 mouse mammary tumor cells, effectively improving survival rates. These findings position taiwaniaquinoids, particularly compound **C36**, as promising therapeutic candidates for human breast cancer.

1. Introduction

Cancer continues to be among the top global causes of mortality, and the incidence continues to rise due to factors such as an aging population, unhealthy lifestyles, and environmental influences. In 2020, lung, liver, stomach, breast, and colon cancers were identified as the most prevalent types and the top five leading causes of cancer-related deaths worldwide [1].

Historically, natural organisms have been used to mitigate numerous diseases, with one potential therapeutic application being the extraction of antitumor or anticancer compounds. Many such compounds are derived from plant species, with several forming part of the standard repertoire of current chemotherapy regimens (such as vincristine, paclitaxel, and epirubicin) [2,3]. Occasionally, a natural product is not the therapeutic agent itself but its derivative. In these instances, the natural compound can serve as a basic scaffold that can be structurally modified to bypass potential issues such as the side effects and undesirable properties of camptothecin and its derivatives [4]. The greater

* Correspondence to: University of Granada, Department of Organic Chemistry, Faculty of Science, C/Fuentenueva s/n, 18071 Granada, Spain.
** Correspondence to: University of Granada, Biopathology and Regenerative Medicine Institute (IBIMER), Centre for Biomedical Research, Avda. del Conocimiento s/n Armilla, 18016 Granada, Spain.
E-mail addresses: rachid@ugr.es (R. Chahboun), fernrs@ugr.es (F. Rodríguez-Serrano).

https://doi.org/10.1016/j.biopha.2023.115791
Received 1 August 2023; Received in revised form 12 October 2023; Accepted 26 October 2023

structural complexity of derivative compounds can in some cases offer an advantage over the original natural products as they tend to exhibit increased selectivity [5,6].

A method for creating bioactive molecules, whether they naturally exist or not, involves using abundant natural products as starting materials for synthesis. These natural precursors often already possess structural characteristics that simplify the synthetic process, allowing complex molecules to be accessed in fewer steps. Numerous examples of this strategy have been reported, including results obtained by our research team, such as the synthesis of meroxest, which boasts a merosesquiterpenic structure [7], and other antitumor agents with a podocarpane and totarane skeleton derived from the natural labdane *trans*-communic acid [8].

Taiwaniaquinoids represent a category of terpenoids that carry the atypical rearranged 5(6→7) or 6-nor-5(6→7) abeo-abietane structure. They have been isolated from certain East Asian conifer species during the past two decades [9]. There have been limited studies offering a brief overview of the biological activities of these compounds. These results indicate that certain compounds display cytotoxic [10–14] and antiparasitic properties [15]. The intriguing biological activity and unique structure of these terpenoids have sparked interest in synthesizing these compounds, including total [16–22] and stereoselective syntheses [23–28]. On the other hand, synthesis beginning with natural terpenoids is highly significant, as it enables the production of enantiopure taiwaniaquinoids in a few steps [29–32]. In our previous study, we evaluated the *in vitro* antiproliferative activity of natural taiwaniaquinoids and associated compounds synthesized from abietic acid (**1**) against breast (MCF-7), lung (A-549) and colon (T-84) cancer cell lines [33]. The results underscored the significant influence of the bromine substituent on C-12 of certain compounds, such as the unnatural taiwaniaquinoids **C15**, **C16**, **C27** and **C36**, which were the most active products (Fig. 1).

The objective of the current study was to elucidate the mechanism underlying the anti-proliferative properties of these taiwaniaquinoids. Given that the greatest efficacy of these compounds was observed in MCF-7 cells, we chose to investigate the mechanisms of action in this tumor line, selecting compound **C36** due to its lower toxicity against healthy peripheral blood mononuclear cells (PBMCs). Additionally, we studied the effects of **C36** on the cell cycle, oxidative stress and apoptosis. A preclinical assay was conducted using murine models to examine the potential *in vivo* implications of the observed *in vitro* antitumor activity, such as liver cytotoxicity and changes in weight or behavior. Finally, we evaluated the effect of **C36** administration in another *in vivo* assay by analyzing the growth and development of tumors in immune-competent C57BL/6 mice implanted with E0771 mouse mammary tumor cells.

2. Results and discussion

2.1. In vitro cytotoxicity assay on PBMCs

To identify the least harmful compound to normal cells among the four taiwaniaquinoids tested (**C15**, **C16**, **C27** and **C36)** with the highest antitumor activity, we assessed their effects by inducing PBMCs. This assay was conducted under the same conditions and concentrations as those used in our previous research against MCF-7, A-549 and T-84 tumor lines [5]. This method, which employs blood cells from healthy donors rather than established human cell lines, as a model to determine the toxicity of certain compounds, has been increasingly used recently [34–36]. The advantageous use of PBMCs stems from their status as "normal" and not "immortalized" cells, in addition to their behavioral similarities with somatic cells in the body [37]. Furthermore, cultured cell lines are susceptible to genetic alterations over several passages, so their use does not guarantee a normal phenotype [38].

Upon evaluating the effect of all tested compounds on PBMCs, the

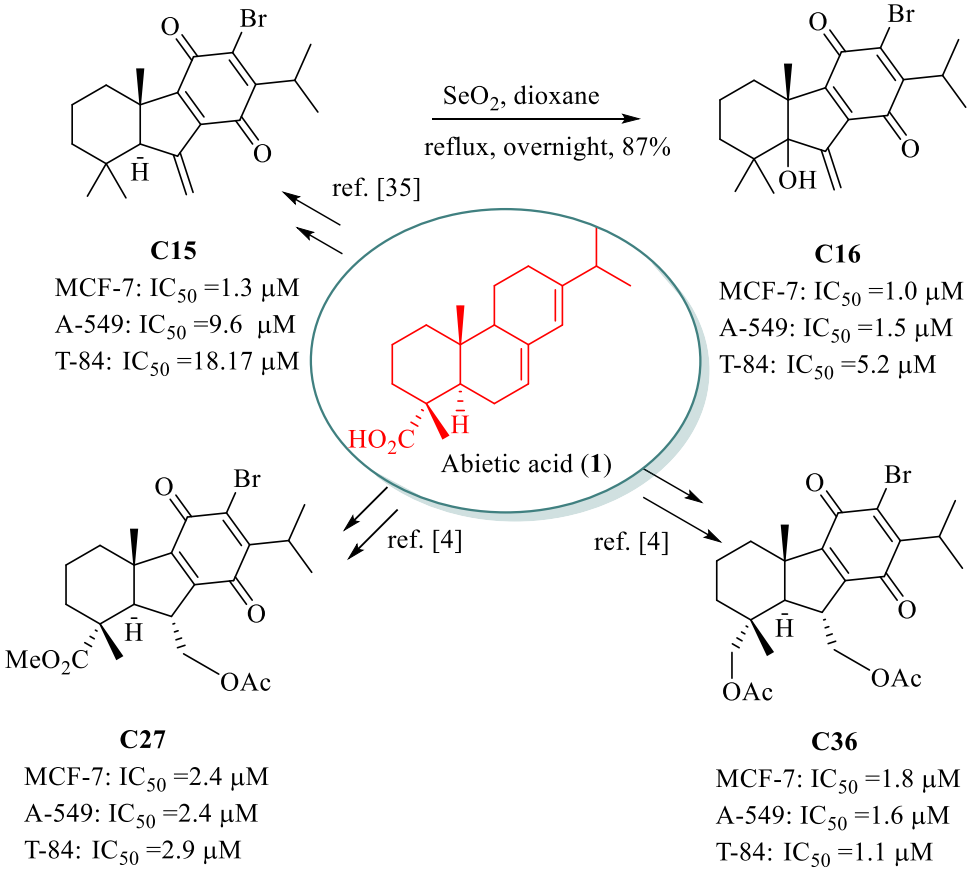

Fig. 1. Chemical structure and IC_{50} of the most active taiwaniaquinoids (C15, C16, C27 and C36) [5].

results indicated that **C36** had an IC_{50} value greater than 20 μM, at least doubling the rest of the IC_{50} values, which were below 10 μM (Fig. 2). Consequently, **C36** appears to be the taiwaniaquinoid that induced the least toxicity in normal cells.

2.2. Oxidative stress induction

The mechanism of action of several antitumor drugs often involves the production of reactive oxygen species (ROS), leading to oxidative imbalance and consequent tumor cell death [39]. Therefore, we decided to test the cytotoxicity of **C36** in MCF-7, A-549 and T-84 tumor lines in the absence and presence of the antioxidant *N*-acetylcysteine (NAC) at 2 mM and investigate whether its mechanism of action was related to ROS production.

Interestingly, we found that the antioxidant NAC significantly influenced the viability of the three tumor cell lines. In the MCF-7 line, at the IC_{50} concentration of **C36**, the percentage of viable cells reached 78.8 % in the presence of NAC and 43.6 % in its absence (Fig. 3). Furthermore, the cytotoxic effect of **C36** was dose dependent; at the $2xIC_{50}$ concentration and in the presence of NAC, **C36** decreased cell viability to 54.3 %, while in the absence of NAC, this percentage dropped to 7.2 %. In T-84 and A-549 cells, there was also a decrease in the cytotoxic activity of **C36** in the presence of NAC, but the percentages were not as high as those in MCF-7 cells. These findings suggest that an antioxidant-rich environment offers cellular protection against the effect of **C36**.

The MCF-7 line was chosen for further testing because the effect of **C36**-induced oxidative stress was more pronounced in this cell line. To confirm these results, we conducted an experiment using DCF-DA dye in the MCF-7 cell line. Cells were treated with the same concentration of **C36**, both with and without 2 mM NAC. The cultures were observed after 1 h of treatment (Fig. 4A). Cells treated with **C36** and NAC were barely stained compared to those treated in the absence of NAC, indicating that the ROS concentration in the latter sample was much higher.

Furthermore, we performed a flow cytometry assay using DCF-DA to evaluate how oxidative stress affected **C36** in MCF-7 cell cultures after 1 h of treatment (Fig. 4B). MCF-7 cells were incubated with and without **C36** (control), and some cultures were treated with H_2O_2 to serve as positive controls.

Our results confirmed that oxidative stress was involved in the mechanism of action of **C36** against these cells. Fig. 4B shows that the highest value of mean fluorescence intensity (MFI) belonged to MCF-7 cells treated with **C36**, reaching 109.0 %, while in the positive control, the MFI value was 52.7 %, and in the control, it was only 16.4 %.

All these data affirm that the cytotoxic activity of **C36** diminishes

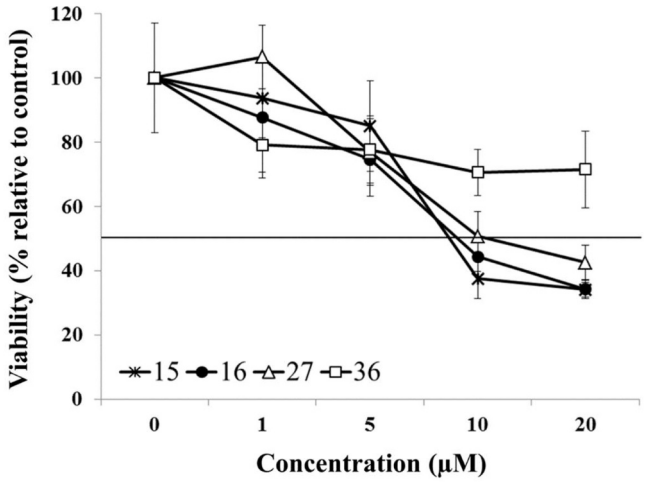

Fig. 2. Effect of compounds C15, C16, C27 and C36 on the viability of PBMCs.

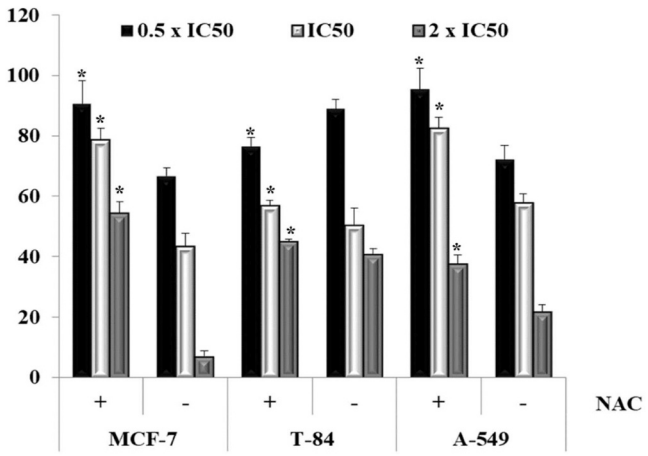

Fig. 3. Viability of MCF-7, T-84 and A-549 cells treated with C36 with or without NAC cotreatment. All cell lines were induced for 72 h at concentrations equivalent to 0.5x, 1x or 2x IC_{50} of C36, with and without 2 mM NAC. The histogram displays the means ± SD of six measurements. IC_{50}: Inhibitory concentration 50.

significantly in the presence of the antioxidant in MCF-7 cells. This demonstrates that oxidative stress is a factor in the mechanism of action of **C36**, similar to other antitumor molecules such as paclitaxel and elesclomol, among others, as reported recently [3,40]. Some studies indicate that the consumption of antioxidant-rich supplements and foods might not be advisable during chemotherapy treatment, and published clinical trial results in this respect have been contentious [41–46].

Intracellular oxidative stress damages both nuclear and mitochondrial DNA, proteins, and membranes. One result of this damage is the modification of DNA bases, such as the oxidation of deoxyguanosine, forming 8-hydroxy-2′-deoxyguanosine (8-OHdG). This is considered a biomarker for evaluating oxidative stress [47,48]. To determine whether our compound induced cellular DNA damage, MCF-7 cells were seeded and either treated or not (control) with **C36** at the IC_{50} concentration for 6 h. All cultures were then stained with anti-8-OHdG and DAPI and observed under fluorescence microscopy (Fig. 5).

2.3. Autophagy assay

Autophagy is a process in which lysosomes merge with autophagic vesicles, leading to the degradation of their contents. Apoptosis and autophagy can mutually enhance or inhibit each other to execute alternative functions within the cell [49,50].

To assess whether the activity of **C36** was related to autophagy, we tested its effect on MCF-7 cells, with and without the autophagy inhibitors chloroquine (CQ) and 3-methyladenine (3-MA). According to our results, 3-MA and CQ did not significantly affect the action of **C36**, which was capable of reducing cell viability in 24 h to below 20 %, with IC_{50} concentration, both in the presence and absence of inhibitors. Therefore, it appears that autophagy is not relevant to the mechanism by which **C36** exerts its cytotoxicity against MCF-7 cells (data not shown). In addition, to corroborate the results with inhibitors, both treated and untreated cells with **C36** were stained with acridine orange (AO) and examined by confocal microscopy (Fig. 6).

After 24 h of induction at IC_{50} and $2xIC_{50}$ concentrations, green color was observed both in the cytoplasm and in the nuclear components of both treated and untreated cells. Some orange-reddish-colored vesicles were also observed, although no differences were found among the cultures. The literature suggests that with compounds that induce autophagy, the quantity of orange vesicles increases proportionally to the dose of the compound [51]. Hence, considering all these results, autophagy is not a mechanism through which **C36** influences MCF-7

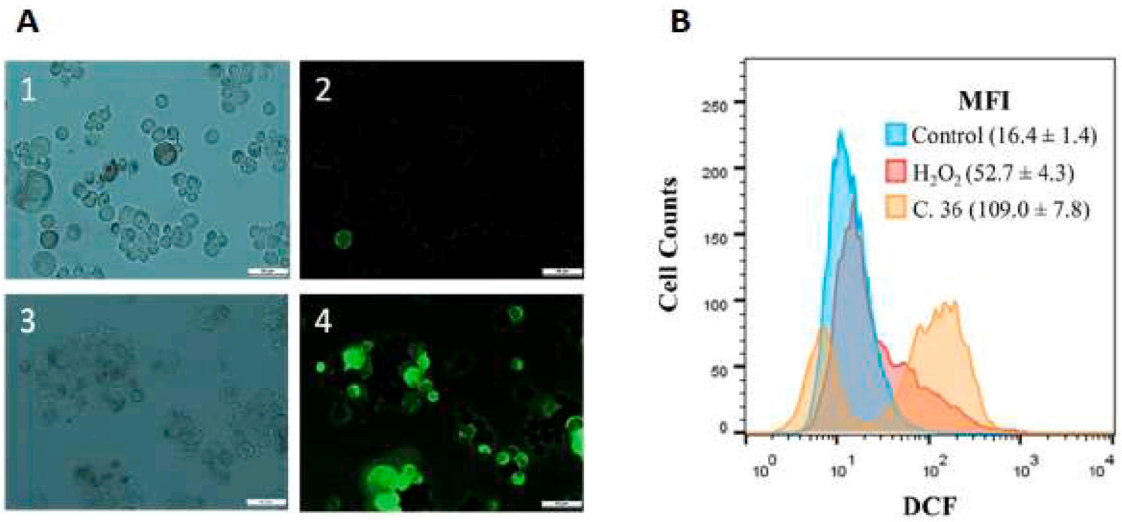

Fig. 4. Analysis of ROS production in MCF-7 cells after 1 h of treatment with C36. (A) Micrograph comparison of MCF-7 cells treated with C36 at the IC_{50} concentration and stained with DCF fluorescence. Bright field micrographs show treated MCF-7 cells either with 2 mM NAC (A1) or without NAC (A3). Micrographs display treated MCF-7 cells either with 2 mM NAC (A2) or without 2 mM NAC (A4). All images were obtained using a fluorescence microscope at 100x magnification. Scale bar represents 60 μm. (B) Cytogram comparing intracellular ROS production, as represented by the MFI, in MCF-7 cells. Cells were stained with DCF-DA and either left untreated (control), treated with C36, or treated with a positive control (H_2O_2).

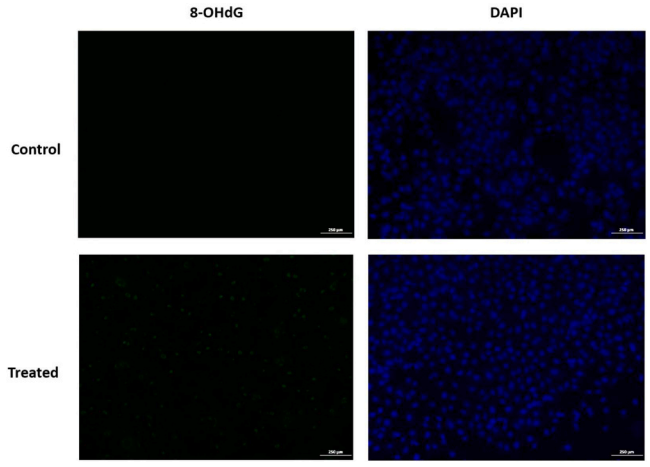

Fig. 5. Immunofluorescence staining of 8-OHdG in MCF-7 cells treated with C36. Top, untreated MCF-7 cells cultured for 6 h (control). Bottom, MCF-7 cells treated with C36 at the IC_{50} concentration (treated) for 6 h. The color blue (DAPI) represents cell nuclei, and the color green (8-OHdG) represents cells that have suffered DNA damage. All images were obtained using a fluorescence microscope at 10x magnification. Scale bar represents 250 μm.

cells.

2.4. Cell cycle analysis

Numerous antitumor agents exhibit an inhibitory effect on tumor development blocking the cell cycle, inducing apoptosis, or having a combined effect on both processes [52–55]. We decided to study whether **C36** was capable of blocking the progression of the cell cycle, as occurs with many natural compounds [56–58]. We carried out this study in three tumor lines: MCF-7, A-549 and T-84.

In MCF-7 cells treated with **C36**, the Sub-G_1 fraction progressively increased with increasing compound concentration compared with control cells after 12 h of induction (Table 1). After 48 h, we observed an increase in this cell population, even with a dose of 0.5xIC_{50}. Therefore, the Sub-G_1 fraction significantly increased in a concentration-responsive manner. The highest percentages of this population (90 % and 86.7 %) were reached at 2xIC_{50} after 24 and 48 h, respectively. Moreover, this Sub-G_1 increase was accompanied by a concomitant decrease in the percentages of G_0-G_1 and S phases compared to the control, especially at IC_{50} and 2xIC_{50} concentrations, after 24 and 48 h of treatment. Regarding the G_2-M phase, this fraction decreased, reaching 1–1.5 %, when cells were incubated with 2xIC_{50} concentration after 24 and 48 h of induction.

In A-549 cells treated with **C36**, the percentage of the Sub-G_1 fraction increased, reaching 40.6 % after 48 h of induction at 2xIC_{50}. The percentages of the other cell cycle phases decreased after 24 and 48 h of induction with IC_{50} and 2xIC_{50} of **C36**. Similarly, in the T-84 line, the most notable data in the Sub-G_1 fraction were after 48 h, at 2xIC_{50} reaching 57.3 %, and the rest of the phases decreased significantly compared to their controls after 24 h of induction at 2xIC_{50}.

Our results showed that in all three cell lines, the Sub-G_1 phase increased as the dose of **C36** and induction time increased, with the MCF-7 line being the most relevant case. These findings suggest DNA degradation, induction of apoptosis and necrosis processes when cells are treated with **C36** at the IC_{50} dose or greater for at least 24 h.

2.5. Apoptosis assays

Programmed cell death can occur mainly through two processes: apoptosis and autophagy. Apoptosis is typified by a succession of morphological transformations, including DNA fragmentation, cell contraction, and the generation of apoptotic bodies that are rapidly phagocytosed by other cells. Autophagy, on the other hand, is characterized by the emergence of autophagosomes that envelop the cytoplasm and cytosolic structures such as mitochondria and endoplasmic reticulum [59,60].

In our study, cultures of MCF-7 cells were induced with two different concentrations of **C36** for 48 h. Using flow cytometry in a viability assay with annexin V-FITC, we determined whether the expanded Sub-G1 cell fraction was a result of induced apoptosis (Fig. 7). Exposure to **C36** decreased the cell viability from 86.3 % (control group) to 45.4 %. This reduction was correlated with an increase in the percentage of apoptotic cells, from 11.6 % in the control group to 49.6 % in samples treated with **C36**, with early apoptosis constituting the highest percentage (45 %). Tumor cells are known to manifest escalated levels of oxidative stress compared with normal cells. Excessive ROS and resulting oxidative

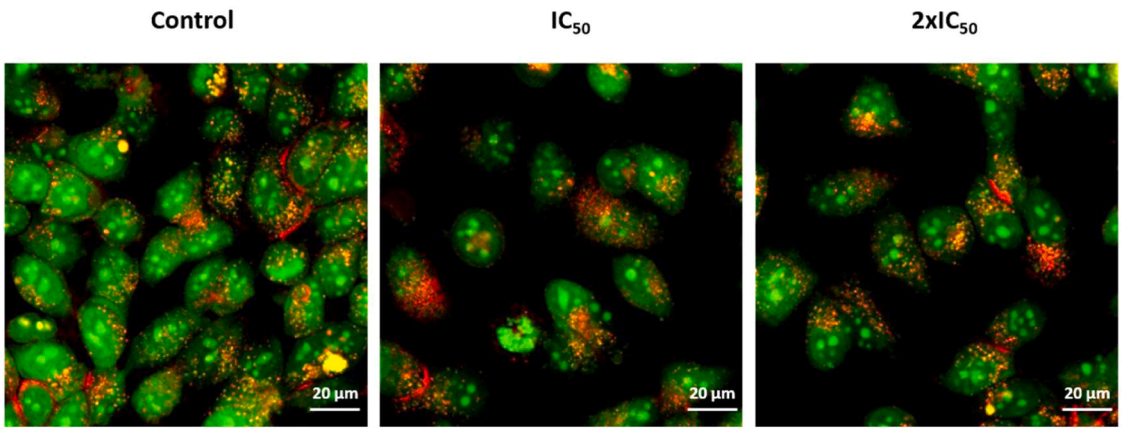

Fig. 6. MCF-7 cells stained with AO after 24 h of induction with vehicle (left; control), IC_{50} C36 (center) or $2xIC_{50}$ C36 (right). Orange vesicles stained with AO represent autophagy. All images were obtained using a confocal microscope at 40x magnification. Abbreviations: AO: acridine orange. Scale bar represents 20 µm.

Table 1
Effects of varying C36 concentrations (0.5x, 1x or 2x IC_{50}) on the cell cycle of MCF-7, A-549, and T-84 cells after 12, 24, and 48 h of induction.

Treatment		MCF-7[a]				A-549[a]				T-84[a]			
		SubG1 (%)	G0-G1 (%)	S (%)	G2-M (%)	SubG1 (%)	G0-G1 (%)	S (%)	G2-M (%)	SubG1 (%)	G0-G1 (%)	S (%)	G2-M (%)
12 h	**Control**	5.94 ± 0.9	78.94 ± 2.1	6.63 ± 1.4	8.49 ± 0.9	1.51 ± 0.1	71.88 ± 1.8	12.00 ± 0.5	14.61 ± 1.3	2.13 ± 0.6	72.70 ± 0.3	14.20 ± 0.3	10.97 ± 0.2
	0.5x	4.27 ± 0.1	77.97 ± 0.5	6.55 ± 1.1	11.20 ± 0.7*	1.71 ± 0.1*	75.63 ± 0.1*	9.56 ± 0.1*	13.10 ± 0.1	1.78 ± 0.1	75.34 ± 0.8*	11.54 ± 0.4*	11.34 ± 1.2
	1x	12.41 ± 0.6*	66.39 ± 0.6*	6.68 ± 0.5	14.52 ± 0.4*	2.30 ± 0.2*	72.05 ± 0.6*	9.85 ± 0.6*	15.80 ± 1.1*	2.34 ± 0.1	75.83 ± 0.4*	10.61 ± 0.6*	11.22 ± 0.4
	2x	60.62 ± 4.2*	28.50 ± 2.8*	5.53 ± 0.6	5.55 ± 1.0*	4.72 ± 0.3*	68.95 ± 0.5*	8.87 ± 0.2*	17.45 ± 1.0*	2.63 ± 0.1	73.53 ± 0.6	10.85 ± 0.3*	12.99 ± 0.7*
24 h	**Control**	5.76 ± 0.3	58.37 ± 1.6	27.08 ± 2.2	8.79 ± 2.0	2.04 ± 1.0	65.79 ± 1.0	12.97 ± 0.8	19.19 ± 0.8	1.28 ± 0.1	68.89 ± 0.5	14.65 ± 0.3	14.18 ± 0.7
	0.5x	6.49 ± 1.2	71.02 ± 1.6*	16.37 ± 1.7*	6.11 ± 1.8*	1.27 ± 0.1*	74.68 ± 1.3	10.44 ± 0.7	13.60 ± 0.5*	1.27 ± 0.1	70.52 ± 1.4*	13.97 ± 0.6	14.24 ± 0.6
	1x	43.04 ± 0.9*	42.03 ± 1.2*	8.07 ± 0.5*	6.86 ± 0.8	3.95 ± 0.4*	77.79 ± 0.1*	7.92 ± 0.8*	10.34 ± 0.5*	1.94 ± 0.2	72.89 ± 0.6*	12.32 ± 0.3*	12.86 ± 0.7*
	2x	90.58 ± 0.1*	6.78 ± 0.4*	1.53 ± 0.4*	1.12 ± 0.1*	16.14 ± 0.8*	61.15 ± 1.3*	7.48 ± 0.2*	15.23 ± 0.7*	16.64 ± 1.0*	61.42 ± 0.5*	9.90 ± 0.4*	12.04 ± 0.3*
48 h	**Control**	3.45 ± 0.7	61.87 ± 2.8	25.57 ± 1.7	9.11 ± 1.6	1.41 ± 0.1	78.78 ± 0.8	7.61 ± 0.5	12.20 ± 0.3	1.84 ± 0.1	79.95 ± 0.3	7.69 ± 0.4	10.52 ± 0.5
	0.5x	4.81 ± 0.6*	71.96 ± 1.4*	18.00 ± 1.4*	5.23 ± 0.5*	2.09 ± 0.1	79.80 ± 0.8	7.46 ± 0.1	10.64 ± 1.1*	2.76 ± 0.1	79.42 ± 0.3	7.74 ± 0.3	10.08 ± 0.5
	1x	51.11 ± 0.7*	30.92 ± 0.3*	8.47 ± 1.2*	9.49 ± 0.6	6.12 ± 0.1*	77.52 ± 0.5*	7.55 ± 0.1	8.81 ± 0.5*	3.99 ± 0.2	79.19 ± 0.5	7.57 ± 0.4	9.25 ± 0.2*
	2x	86.71 ± 1.8*	8.72 ± 1.5*	3.04 ± 0.7*	1.54 ± 0.1*	40.64 ± 0.1*	47.39 ± 0.3*	3.78 ± 0.4*	8.19 ± 0.1*	57.34 ± 3.0*	31.70 ± 1.5*	6.39 ± 1.1*	4.56 ± 0.4*

[a] Data are means ± SD of three independent determinations.
* Indicates a significant difference from the control group, with a p value of < 0.05.

stress are linked to metabolic changes related to oncogenic transformation and play a central role in apoptosis-induced cell death [61,62].

Consequently, tumor cells may be particularly sensitive to agents that either significantly elevate ROS levels or impair the cell ability to neutralize ROS [63]. Apoptosis, or programmed cell death, is driven by a class of proteases called caspases. These enzymes initiate signaling cascades that culminate in DNA fragmentation and microtubule disruption [64,65].

The data suggest that **C36** affects MCF-7 cells by generating oxidative stress and inducing apoptosis. This mechanism mirrors that of other reported molecules, such as certain merosquiterpenoids [66], supercinnamaldehyde (SCA) compounds [67], some chromenopyrazolediones [68] and acetylsalicylic acid [69,70]. Apoptosis can occur through either the extrinsic or intrinsic pathway. The extrinsic pathway is activated by a death receptor, leading to caspase 8 activation, which is subsequently followed by caspase 3 activation. The intrinsic pathway is activated by cellular stress signals that originate in the mitochondria and are regulated by Bcl-2 family proteins. These proteins can either promote or inhibit apoptosis, such as Bax and Bcl-2, respectively [8,71,72]. In MCF-7 cells induced with **C36**, there was a notable increase in Bax protein expression at 3 h, particularly at $2xIC_{50}$, but this expression decreased at 6 h. Conversely, the Bcl-2 protein expression decreased over the 6 h postinduction (Fig. 8A).

The caspase family proteins include initiators such as caspases 8, 10, 2, and 9, and later effectors like caspases 3, 6, and 7 [73,74]. Notably, MCF-7 cells are reported to lack expression of caspase 3 [75]. It is hypothesized that these cells induce apoptosis through a sequential activation of caspases 9, 7, and 6 [76].

Considering this and based on our Bcl-2 and Bax results, we examined the levels of caspase 9 in MCF-7 cells, given its significance as a key initiator of the intrinsic pathway. After induction with the IC_{50} of **C36**, cleaved caspase 9 bands were observed at both 3 and 6 h (Fig. 8B). These findings suggest that **C36** promotes apoptosis in MCF-7 cells via its

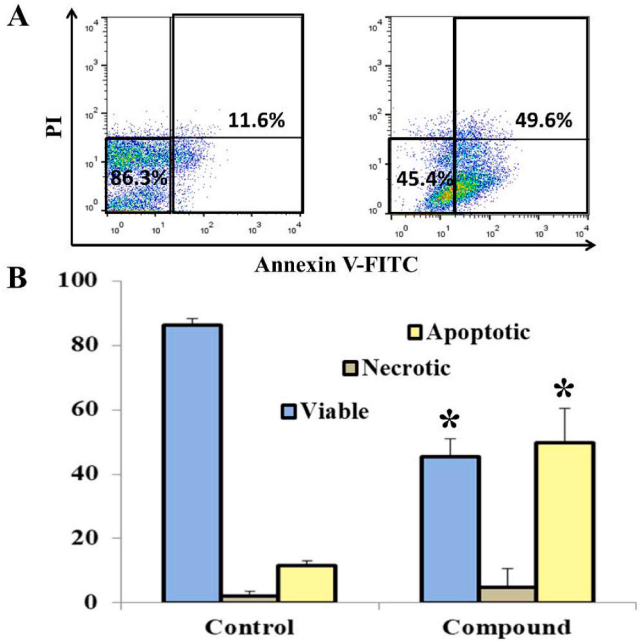

Fig. 7. Annexin V-FITC/PI Staining for Apoptosis and Viability Assessment. Flow cytometric analysis was performed on MCF-7 cells treated with or without C36 for 48 h. A) Cytograms depicting untreated (control, left) and C36-treated (right) MCF-7 cell cultures. This experiment was independently replicated three times, all leading to similar results. B) Histograms displaying the proportion of viable, necrotic and apoptotic MCF-7 cells after 48 h, highlighting the differences between the control group and cells exposed to C36 at the IC_{50} concentration.

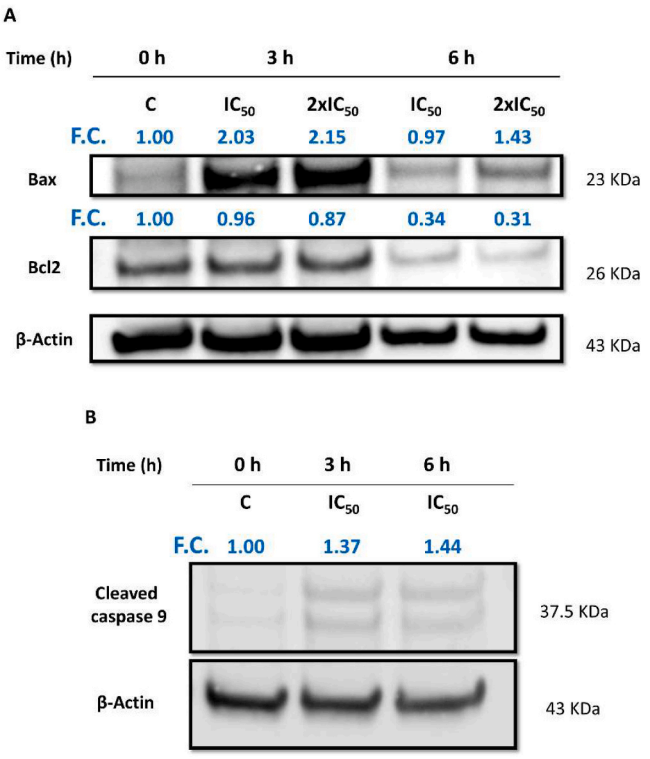

Fig. 8. Immunoblot evaluation of apoptosis markers. A) Expression of Bax and Bcl-2 in MCF-7 cells, uninduced (control; C) and induced with C36 at IC_{50} and $2xIC_{50}$ concentrations for 3 and 6 h. B) Expression of cleaved caspase 9 in MCF-7 cells, uninduced (control; C) and induced with C36 at IC_{50} concentrations for 3 and 6 h. Densitometry values (blue numbers) represent fold change (F.C.) of the relative protein expression compared to control.

intrinsic pathway. This mechanism is similar to those exhibited by other compounds evaluated for their effect on breast tumor cells [76–79]. Furthermore, a study involving resveratrol revealed that the mitochondrial caspase-9 pathway was the primary apoptotic pathway implicated in MCF-7 cells [80].

2.6. *In vivo toxicity assay*

To evaluate the toxicity of **C36**, we conducted an *in vivo* assay in mice, considering changes in body weights, and performed hematological, biochemical, and histopathological analyses following treatment with the compound. The control group was administered solely with the vehicle, 0.5 % methylcellulose (MC), while the other four groups of C57BL/6 mice received increasing doses of **C36** (1.75, 5.5, 17.5, or 55 mg/kg) over a 22-day study period. All mice were weighed twice weekly.

Generally, all mouse groups demonstrated a consistent gain in body weight from the beginning to the end of the study period (Table 2). No differences were observed between the weights of the five groups on either day 1 ($P = 0.541$) or day 22 ($P = 0.096$). Both initial and final body weights on day 1 and day 22, respectively, did not show significant differences among the five groups, and the final weight percentages relative to controls were comparable across all groups. Our results indicated no variation in body weight among the animals throughout the study. Furthermore, **C36** treatment was not associated with any behavioral alterations, diarrheal episodes, or other adverse effects.

Hematological analyses were conducted using blood samples obtained after the 22-day treatment. The results demonstrated normal levels of leukocytes, red blood cells and hemoglobin compared to those in the control group (Table 3). Furthermore, conditions such as anemia, leukopenia, thrombocytopenia, or pancytopenia were not detected in mice receiving **C36**.

In the course of this investigation, we carried out biochemical assessments examining glucose and total protein concentrations in the blood following treatment with the aim of gauging the general health status of the mice. Neither glucose nor total protein levels showed substantial variations across the different groups (Table 4).

Urea and creatinine served as markers of renal function in our study. Urea is a metabolic product, whereas creatinine is related to the degradation of muscle tissue. Elevation in either of these markers can hint at renal dysfunction, with urea reflecting an acute condition and creatinine indicating a chronic state. Nevertheless, our study revealed no marked differences in the levels of either marker across the groups, thereby suggesting that **C36** did not induce renal toxicity (Table 4).

Bilirubin, a compound employed by the liver for the synthesis of bile, is typically present in trace amounts in the blood. Following treatment, no variations were discerned in total bilirubin levels. Similarly, the

Table 2
Comparative body weights of untreated (control) and C36-treated C57BL/6 mice.

Concentration (mg/kg body weight)	Survival	MBW (g)		Final Weight Relative to Controls (%)
		Initial	Final	
0 (Control)	2/2	16.8 ± 0.9	18.3 ± 1.1	100.0
1.75 (Group 1)	2/2	18.2 ± 2.0	20.3 ± 1.3	110.9
5.5 (Group 2)	2/2	18.3 ± 0.9	19.9 ± 1.0	108.7
17.5 (Group 3)	2/2	18.0 ± 0.8	19.2 ± 1.0	104.9
55 (Group 4)	2/2	17.1 ± 0.8	19.3 ± 1.0	105.5

Table 3
Hematological Impact of C36. Comparative hemogram results from untreated and C36-treated C57BL/6 mice, presented at the endpoint of the 22-day experimental period.

Parameters	Control (vehicle)	Group 1 (1.75 mg/kg)	Group 2 (5.5 mg/kg)	Group 3 (17.5 mg/kg)	Group 4 (55 mg/kg)
WBC (10^3/μl)	5.0 ± 0.6	5.4 ± 1.6	5.0 ± 0.6	5.3 ± 1.0	5.7 ± 0.6
RBC (10^6/μl)	8.9 ± 0.2	8.7 ± 0.4	8.8 ± 1.0	9.2 ± 0.0	8.7 ± 0.3
HGB (g/dL)	13.8 ± 0.4	7.1 ± 9.5	14.0 ± 0.0	14.7 ± 0.0	13.9 ± 0.6
HCT (%)	41.6 ± 1.8	40.9 ± 0.5	40.6 ± 1.0	42.4 ± 1.0	40.7 ± 2.0
PLT (10^3/μl)	531.5 ± 116.7	516.0 ± 9.9	657.5 ± 51.6	583.0 ± 58.0	664.5 ± 67.2
MCV (fL)	46.4 ± 0.6	47.0 ± 1.6	46.1 ± 0.3	46.3 ± 0.1	47.1 ± 1.3
MCH (pg)	15.4 ± 0.0	16.1 ± 1.0	15.9 ± 0.1	16.0 ± 1.0	16.1 ± 0.3
MCHC (g/dL)	33.1 ± 0.3	34.3 ± 1.1	34.4 ± 1.0	34.6 ± 1.0	34.3 ± 0.1
MPV (fL)	5.8 ± 0.3	5.9 ± 0.1	5.6 ± 1.0	6.1 ± 0.6	6.0 ± 0.1
RDW (%)	13.8 ± 0.3	14.5 ± 1.0	14.1 ± 0.1	13.8 ± 0.8	14.3 ± 0.3
PCT (%)	0.3 ± 1.0	0.3 ± 0.0	0.3 ± 0.0	0.2 ± 0.2	0.4 ± 0.0
LYM (%)	95.4 ± 1.2	94.0 ± 1.4	95.5 ± 2.0	95.0 ± 0.1	94.0 ± 1.0
MON (%)	0.2 ± 1.0	0.3 ± 1.0	0.1 ± 1.0	0.2 ± 0.0	0.3 ± 0.1
NEU (%)	3.9 ± 0.8	5.1 ± 1.2	3.9 ± 2.0	4.4 ± 0.3	5.1 ± 0.7
EOS (%)	0.1 ± 0.2	0.2 ± 0.0	0.1 ± 0.1	0.2 ± 0.1	0.2 ± 0.2
BAS (%)	0.2 ± 1.0	0.2 ± 0.1	0.3 ± 0.2	0.2 ± 0.0	0.3 ± 0.2

Data are presented as the mean ± S.D. Abbreviations: WBC, white blood cells (10^3/μl); RBC, red blood cells (10^6/microliter); HGB, hemoglobin; HCT, hematocrit; PLT, platelets; MCV, mean corpuscular volume; MCH, mean corpuscular hemoglobin; MCHC, mean corpuscular hemoglobin concentration; MPV, mean platelet volume; RDW, red cell distribution width; PCT; LYM, lymphocytes; MON, monocytes; NEU, neutrophils; EOS, eosinophils; BAS, basophils.

quantities of alanine transaminase, an enzyme predominantly found in liver cells that typically sees a surge in blood concentration subsequent to liver cell injury or necrosis, showed no marked differences in the treated groups compared to the control. These observations collectively suggest that **C36** did not induce significant liver toxicity (Table 4).

Despite the relatively small sample size for each group, the results from the analysis presented in Tables 2, 3, and 4 were pivotal for our toxicity study. They provided us with the capacity to identify any potential hematological and biochemical changes in the mice subjected to **C36** treatment, should they exist.

We conducted a histological study to compare liver samples from the control group mice to those treated with the maximum administered dose of **C36** (55 mg/Kg). From a pathological standpoint, neither abnormalities nor histopathological changes (hepatocyte degeneration, fat accumulation or nuclear alterations) were observed under a microscopic examination.

Minimal hepatocyte ballooning was detected in the samples from treated mice, a phenomenon that has been observed in other studies without resulting in liver toxicity [81–83]. Collectively, these histological findings suggest that C36 treatment did not induce significant toxic effects in the liver, an inference supported by the blood analysis data that demonstrated normal total bilirubin and alanine aminotransferase levels (Fig. 9). The findings in this section point to a high level of tolerance to **C36**.

2.7. *In vivo tumor assay*

The promising outcomes from the *in vitro* and *in vivo* toxicity tests prompted us to further explore the impact of **C36** on tumor development *in vivo*. For this study, we selected the E0771 cell line due to its similar characteristics to the MCF-7 line used in our previous *in vitro* experiments, where the IC_{50} value of **C36** was 1.8 μM in MCF-7 cells [5]. The E0771 line, originally derived from a breast tumor in a C57BL/6 mouse, facilitates the formation of rapidly growing tumors in immune-competent mice of the same strain. This syngeneic allograft model involving C57BL/6 mice and E0771 cells offers a more clinically relevant scenario for translational studies. Furthermore, in alignment with the 3Rs principles, we used a minimally sufficient sample size for this study to allow for the detection of any potential *in vivo* antitumor effects of **C36** [84]. Prior to this *in vivo* investigation, we assessed the cytotoxicity of **C36** in E0771 cells and determined an IC_{50} value of 1.39 μM.

An exponentially growing suspension of E0771 cells (1 $\times 10^6$ cells) was injected into the subcutaneous tissue in the right flank of each animal to induce tumor growth [66]. When tumors became palpable (day

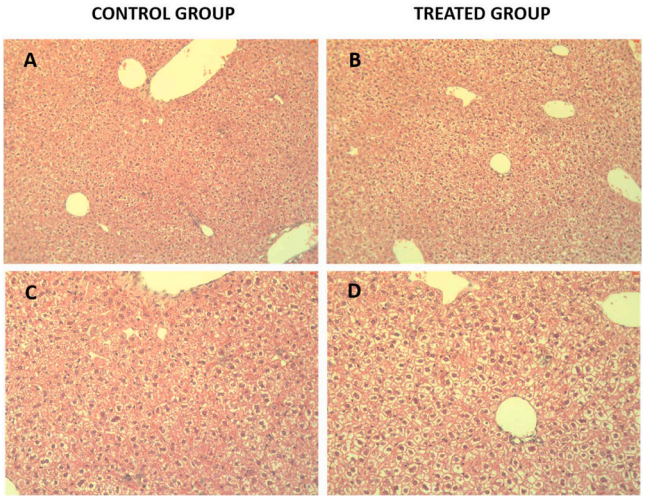

Fig. 9. Histological evaluation of mouse liver sections. Bright-field optical microscopy images of liver sections stained with hematoxylin and eosin (H&E). Images A and C were derived from control group mice, while images B and D were obtained from mice treated with 55 mg/Kg of C36. Magnifications were 10x (A and B) or 20x (C and D).

Table 4
Influence of C36 on the clinical blood biochemistry of C57BL/6 Mice.

	Parameters	Control (vehicle)	Group 1 (1.75 mg/kg)	Group 2 (5.5 mg/kg)	Group 3 (17.5 mg/kg)	Group 4 (55 mg/kg)
Overall Status	**GLU** (mg/dL)	283.2 ± 15.5	220.0 ± 32.8	201.2 ± 5.8	257.5 ± 18.4	256.3 ± 10.4
	T. PROTEIN (g/dL)	4.7 ± 0.3	5.6 ± 0.6	4.6 ± 0.5	5.1 ± 0.4	4.7 ± 0.6
Kidney Toxicity	**BUN** (mg/dL)	48.2 ± 7.8	42.1 ± 3.8	46.2 ± 0.3	53.0 ± 15.5	46.5 ± 3.0
	CRE (mg/dL)	0.3 ± 0.0	0.4 ± 0.0	0.3 ± 1.0	0.2 ± 0.3	0.4 ± 0.1
Liver Toxicity	**T. BIL** (mg/dL)	1.4 ± 0.0	2.2 ± 1.2	1.4 ± 0.0	1.4 ± 0.0	1.7 ± 0.4
	ALT (U/L)	37.3 ± 16.4	36.3 ± 15.9	26.0 ± 3.4	35.0 ± 1.8	32.0 ± 9.3

Data are reported as the mean ± S.D. Abbreviations: GLU, glucose; T. Protein, total protein; BUN, blood urea nitrogen; CRE, creatinine; T. BIL, total bilirubin; ALT, alanine aminotransferase.

8), the mice were randomly divided into two groups of seven. Animals received oral treatment twice a week (on postinjection days 8, 11, 14, 17, 21, 24, 28, and 31) with either the 1 % methylcellulose vehicle alone (control), or with **C36** at a concentration of 55 mg/kg bw (treated). The study was concluded on day 33, by which time all mice in the control group had either succumbed or met the endpoint criterion. Notable differences in tumor sizes between the two groups were observed starting from the fifth oral administration of **C36** (day 21). In the control group, the mean tumor size was double that of the treated group by day 24, and this disparity grew to nearly fivefold by day 28 (Fig. 10A).

Remarkably, by day 33, while no mice survived in the control group, four treated animals were still alive. A significant difference in survival rates was identified based on the log-rank test (Fig. 10B). These results compellingly demonstrate the *in vivo* antitumor efficacy of **C36**.

3. Conclusions

Our previous studies have highlighted the *in vitro* antitumor potential of taiwaniaquinoids. However, their mechanism of action or *in vivo* toxicity or efficacy has not been explored. In the present study, we selected the most potent taiwaniaquinoids against human breast, lung, and colon cancer cells (**C15**, **C16**, **C27** and **C36**), with a specific focus on MCF-7 cells and **C36**, as they displayed the highest effectiveness and lowest toxicity against normal PBMCs. Through multiple *in vitro* assays, we demonstrated that **C36** induces oxidative stress and triggers apoptosis via the intrinsic pathway in tumor cells. Furthermore, **C36** was shown to inflict DNA damage and incite apoptosis in tumor cells, as evidenced by the detection of specific markers. The *in vivo* toxicity study revealed that **C36** administration up to 55 mg/kg bw did not significantly affect body weight, behavior, blood parameters, or liver tissue in immunocompetent C57BL/6 mice. Remarkably, in our *in vivo* tumor model that involved C57BL/6 mice and E0771 cell allografts, **C36** intake both suppressed tumor progression and significantly extended survival. While further studies are needed, our findings suggest that taiwaniaquinoids, particularly **C36**, exhibit promising potential for cancer therapy given their low systemic toxicity and strong antitumor effects. This indicates the potential of taiwaniaquinoids, specifically **C36**, as compelling candidates for clinical trials in cancer treatment.

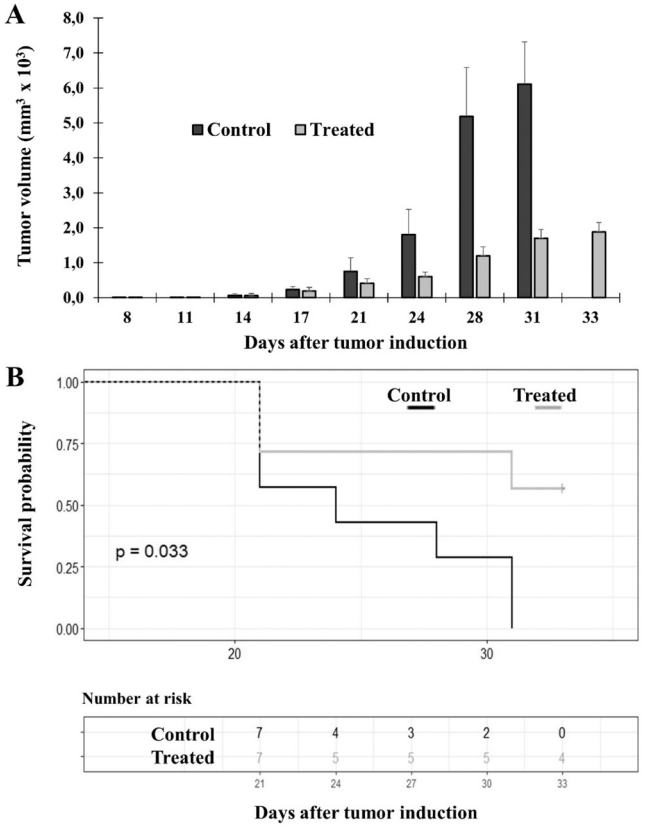

Fig. 10. Effect of C36 on a breast cancer model involving C57BL/6 mice and E0771 cells: progression of breast tumor size (A) and survival curve (B).

4. Experimental section

4.1. Cell lines and culture

For the *in vitro* assays, we used the human breast adenocarcinoma line MCF-7, human lung tumor line A-549, human colorectal carcinoma line T-84, and the E0771 breast cancer cell line that was isolated from an immunocompetent C57BL/6 mouse. All cells were cultured in DMEM, supplemented with 10 % heat-inactivated FBS and penicillin-streptomycin. Cultures were kept in a humidified atmosphere of 5 % CO_2 at 37ºC. All the necessary culture media and supplements were procured from Sigma-Aldrich (St. Louis, MO).

4.2. In vitro antiproliferative assay with PBMCs

PBMCs were obtained from peripheral blood samples from healthy donors that were obtained through the Biobank of the Public Health System of Andalusia (Spain). The cells were isolated from blood by density-gradient centrifugation using Histopaque-1077 (Sigma Aldrich). The PBMCs were cultivated in RPMI-1640 medium supplemented with 20 % FBS, 2 mM glutamine, and penicillin-streptomycin, and were maintained in a humidified atmosphere of 5 % CO_2 at 37ºC. To calculate the IC_{50}, we seeded 5×10^4 cells in each well of 96-well plates in sextuplicate that were treated with the taiwaniaquinoids showing the highest activities in previous studies (compounds **C15**, **C16**, **C27** and **C36**) at various concentrations (1–20 μM) for 72 h. Cell viability was assessed using the MTT assay (Sigma-Aldrich), and optical density was measured at 570 nm using a spectrophotometer (Multiskan EX, Thermo).

4.3. Oxidative stress and DNA damage assays

To ascertain the impact of oxidative stress on the antiproliferative effect of **C36** on MCF-7 cells, 2×10^3 cells were seeded in sextuplicate in each well of a 96-well plate. Following 24 h, cells were treated with incrementally increasing concentrations of **C36**, with or without an antioxidant (NAC, Trolox, or BHA) added 1 h before the compound, and incubated for 72 h. After treatment, cells were fixed with 10 % cold trichloroacetic acid (4 °C), stained with 0.4 % sulforhodamine B in 1% acetic acid, and then the dye was dissolved in 10 mM Tris-base pH 10.5. Optical density was measured at 492 nm using a spectrophotometer (Multiskan EX, Thermo). IC_{50} values were derived from the semi-logarithmic dose-response curve by linear interpolation. Concurrently, intracellular ROS levels were evaluated using a FACScan flow cytometer (Becton Dickinson, San Jose, CA, USA), through the quantification of fluorescence intensity after 30 min incubation with 2′,7′-dichlorofluorescein diacetate (DCF-DA, Sigma-Aldrich). Furthermore, MCF-7 cells were plated in microslide-well dishes (IBIDI) with **C36** at a concentration equivalent to IC_{50}, incubated for 1 h in the presence or absence of 2 mM NAC and then incubated with DCF- DA for an additional 30 min. Finally, the cells were rinsed with PBS and visualized using fluorescence microscopy (Leica DM5500B; Leica, Germany) at 100x magnification.

To evaluate DNA damage, MCF-7 cells were seeded in microslide-well dishes (IBIDI) and incubated overnight. Subsequently, the cells were exposed to **C36** at the IC_{50} concentration for 6 h. After treatment, the cells were fixed with 4 % paraformaldehyde in PBS for 10 min, and then permeabilized with 0.25 % Triton X-100 in PBS for an extra 10 min. After washing three times in PBS for 5 min each, the cells were

incubated in 5 % BSA in PBS for 1 h and then with primary antibody 8-OHdG-FITC (Santa Cruz Biotechnology) at 4 °C overnight. The cells were then rinsed with PBS and incubated with the secondary antibody m-IgGk-BP-FITC (Santa Cruz Biotechnology) for 1 h. Finally, the cells were washed with PBS, stained with DAPI (1 μg/mL) for 1 min, gently washed with PBS, and then observed under a fluorescence microscope.

4.4. Autophagy assays

The effects of **C36** were assessed with or without a 1-h pretreatment with one of the autophagy inhibitors, 3-MA or CQ. For this, we seeded MCF-7 cells in 96-well plates or μslide-well dishes (IBIDI). Following the induction period, the 96-well plates underwent cell quantification via sulforhodamine B staining as outlined in Section 4.3. The μslide-well dishes were stained with 1 μM acridine orange (Sigma-Aldrich, A318337) at 37 °C for 15 min, rinsed with distilled water, and examined under a fluorescence microscope to identify the presence of acidic intracellular compartments.

4.5. Cell cycle and sub-G1 analysis

To assess the impact of **C36** on the cell cycle, MCF-7 cells were plated in 6-well plates and then cultured for 12 h in serum-free medium. After this period, the cells were incubated in complete medium with or without **C36** for 12, 24, or 48 h. Following this, cultures were harvested, rinsed with PBS, fixed with 70 % cold ethanol, and treated with a DNA extraction solution (0.2 M Na_2HPO_4, 0.1 M citric acid) for 15 min at 37 °C. The cells were subsequently centrifuged, rinsed with PBS, resuspended in a solution containing propidium iodide (40 μg/mL) and RNase (100 μg/mL), and then incubated for 30 min at 37 °C in the dark. Finally, the cells were examined using a FACScan flow cytometer.

4.6. Viability and apoptosis assays

MCF-7 cultures induced or not with **C36** were used to analyze cell viability employing the Annexin V-FITC kit (Trevigen, Gaithersburg, MD), according to the protocol described in [10]. Additionally, the level of apoptosis-related markers in cultures treated or not treated with the compound was assayed by western blot following the protocol described in [10]. In these assays, we used the primary antibodies anti-Bcl2 (SC-56015, Santa Cruz), anti-Bax (Santa Cruz) and anti-cleaved caspase-9 (Cell Signaling), and the secondary antibody were m-IgG kappa BP-HRP (Santa Cruz) or IgG HRP-conjugate (Sigma-Aldrich). β-actin served as a housekeeping reference and was detected using monoclonal anti-β-actin-HRP (Sigma-Aldrich).

4.7. In vivo assays

The *in vivo* assays were approved by the Ethics Committee of the University of Granada. (Ethical consent approval Nº: 49-CEEA-OH-2014). The animals were housed in cages with unrestricted access to water and rodent laboratory chow, and were maintained under a controlled environment (12 h light/dark cycle, 37 °C, 40–70 % relative humidity). To determine the *in vivo* toxicity of **C36**, ten female C57BL/6 mice weighing 25–30 g were randomly divided into five groups (n = 2). The control group was treated with vehicle (1 % methylcellulose solution), and the other four groups were administered **C36** at different concentrations (1.75, 5.5, 17.5 and 55 mg/Kg) seven times over the course of a 22-day assay. Throughout the study, mice were observed for signs of toxicity, including loss or changes in coat and behavior, diarrhea, and loss of movement or weight. The mice were weighed twice weekly during the experimental period.

At the end of the assay blood was drawn from each mouse, and plasma was extracted for the analysis of hematological and biochemical parameters: white blood cells, red blood cells, hemoglobin, hematocrit, mean corpuscular volume, mean corpuscular hemoglobin, mean corpuscular hemoglobin concentration, platelets, mean platelet volume, red cell distribution width, platelet distribution width, neutrophils, lymphocytes, monocytes, eosinophils, basophils, glucose, total protein, blood urea nitrogen, creatinine, total bilirubin and alanine aminotransferase. In addition, liver tissue was collected from each mouse, fixed in neutral buffered formalin, and embedded in paraffin. Five-micron sections were stained with hematoxylin and eosin and examined by optical microscopy using a Leica DM IL LED microscope (Leica Microsystems S.L.U., Barcelona, Spain).

For the *in vivo* tumor assay, fourteen female C57BL/6 mice weighing 25–30 g were injected with 1×10^6 E0771 cells to induce tumors. Once the tumors became palpable, animals were randomly divided into two groups: a control group administered vehicle alone (0.5 % methylcellulose) and a treatment group administered 55 mg/kg bw **C36**. Oral administration and tumor measurements were conducted twice weekly. Tumor dimensions were measured using a digital caliper. The largest diameter (a) and the second largest diameter (b), perpendicular to the former, were recorded. Tumor volume (V, mm^3) was estimated using the formula: $V = a \cdot b^2 \cdot \pi/6$.

4.8. Statistical analysis

Quantitative results are reported as the mean ± standard deviation. Depending on the data distribution, comparisons were made using either parametric (Student's t test or ANOVA) or nonparametric (Mann-Whitney U test or Kruskal-Wallis H test along with Dunn's post-hoc test) statistical tests. Survival probabilities were computed using the Kaplan-Meier method, with the significance of the results calculated using the log-rank test. All statistical analyses were conducted using SPSS (v. 28). A p value below 0.05 was deemed to represent statistical significance.

CRediT authorship contribution statement

Conceptualization: **R.C., E.A.M., F.R.S.,** and **N.M.S.,;** Formal analysis: **N.M.S., H.Z. I.B.,** and **F.R.S.;** Funding acquisition: **E.A.M., R.C.,** and **F.R.S.;** Investigation: **N.M.S., J.J.G., F.J.,** and **F.J.R.-Z.;** Methodology: **F.R.S., R.C., N.M.S., I.B., A.F.** and **J.M.G.;** Project administration: **E.A.M., F.R.S, and R.C.;** Resources: **E.A.M., F.R.S,** and **R.C.;** Supervision: **R.C., J.A.L.** and **F.J.R.-Z;** Validation: **N.M.S., H.Z., F.R.S., I.B., A.F., and J.M.G.;** Visualization: **N.M.S., H.Z., A.F., I.B.,** and **F.R.S.;** Writing – original draft: **N.M.S, R.C.,** and **F.R.S.;** Writing – review & editing: **N.M.S. R.C.,** and **F.R.S.**

Declaration of Competing Interest

The authors declare that they have no known competing financial interests or personal relationships that could have appeared to influence the work reported in this paper.

Acknowledgements

This work was supported by grants from the Consejería de Salud y Familias - Junta de Andalucía (PECART-0207-2020), the Junta de Andalucía - Universidad de Granada - European Regional Development Fund (B-FQM-278–UGR20), and the Ministerio de Economía y Competitividad (CTQ2014-56611-R).

References

[1] W. Cao, H.-D. Chen, Y.-W. Yu, N. Li, W.-Q. Chen, Changing profiles of cancer burden worldwide and in China: a secondary analysis of the global cancer statistics 2020, Chin. Med J. 134 (2021) 783–791, https://doi.org/10.1097/CM9.0000000000001474.

[2] D.J. Newman, G.M. Cragg, Natural products as sources of new drugs from 1981 to 2014, J. Nat. Prod. 79 (2016) 629–661, https://doi.org/10.1021/acs.jnatprod.5b01055.

[3] R.C. Alves, R.P. Fernandes, J.O. Eloy, H.R.N. Salgado, M. Chorilli, Characteristics, properties and analytical methods of paclitaxel: a review, Crit. Rev. Anal. Chem. 48 (2018) 110–118, https://doi.org/10.1080/10408347.2017.1416283.

[4] E. de, L. Chazin, R. da, R. Reis, W.T.V. Junior, L.F.E. Moor, T.R.A. Vasconcelos, An overview on the development of new potentially active camptothecin analogs against cancer, Mini Rev. Med. Chem. 14 (2014) 953–962.

[5] J.J. Guardia, R. Tapia, S. Mahdjour, F. Rodriguez-Serrano, N. Mut-Salud, R. Chahboun, E. Alvarez-Manzaneda, Antiproliferative activity of natural Taiwaniaquinoids and related compounds, J. Nat. Prod. 80 (2017) 308–318, https://doi.org/10.1021/acs.jnatprod.6b00700.

[6] I. Robles-Fernández, F. Rodríguez-Serrano, P.J. Álvarez, R. Ortiz, A.R. Rama, J. Prados, C. Melguizo, E. Álvarez-Manzaneda, A. Aránega, Antitumor properties of natural compounds and related molecules, Recent Pat. Anticancer Drug Discov. 8 (2013) 203–215.

[7] E. Carrasco, J.M. Garrido, P.J. Álvarez, E. Álvarez-Manzaneda, R. Chahboun, I. Messouri, C. Melguizo, A. Aránega, F. Rodríguez-Serrano, Meroxest improves the prognosis of immunocompetent C57BL/6 mice with allografts of E0771 mouse breast tumor cells, Arch. Med. Sci. 12 (2016) 919–927, https://doi.org/10.5114/aoms.2014.45442.

[8] S. Mahdjour, J.J. Guardia, F. Rodríguez-Serrano, J.M. Garrido, I.B. López-Barajas, N. Mut-Salud, R. Chahboun, E. Alvarez-Manzaneda, Synthesis and antiproliferative activity of podocarpane and totarane derivatives, Eur. J. Med. Chem. 158 (2018) 863–873, https://doi.org/10.1016/j.ejmech.2018.09.051.

[9] G. Majetich, J.M. Shimkus, The taiwaniaquinoids: a review, J. Nat. Prod. 73 (2010) 284–298, https://doi.org/10.1021/np9004695.

[10] M. Iwamoto, H. Ohtsu, H. Tokuda, H. Nishino, S. Matsunaga, R. Tanaka, Anti-tumor promoting diterpenes from the stem bark of Thuja standishii (Cupressaceae), Bioorg. Med. Chem. 9 (2001) 1911–1921.

[11] T. Minami, M. Iwamoto, H. Ohtsu, H. Ohishi, R. Tanaka, A. Yoshitake, Aromatase inhibitory activities of standishinal and the diterpenoids from the bark of Thuja standishii, Planta Med 68 (2002) 742–745, https://doi.org/10.1055/s-2002-33787.

[12] J.R. Hanson, Diterpenoids, Nat. Prod. Rep. 21 (2004) 312–320, https://doi.org/10.1039/B300377A.

[13] C.-I. Chang, J.-Y. Chang, C.-C. Kuo, W.-Y. Pan, Y.-H. Kuo, Four new 6-nor5(6–>7) abeo-abietane type diterpenes and antitumoral cytotoxic diterpene constituents from the bark of Taiwania cryptomerioides, Planta Med. 71 (2005) 72–76, https://doi.org/10.1055/s-2005-837754.

[14] A. Aránega Jiménez, E. Álvarez-Manzaneda, R. Chaboun Karimi, F. Rodríguez Serrano, J.C. Prados Salazar, C. Melguizo Alonso, R. Tapia Martín, H. Es-Samti, J.J. Guardia Monteagudo, M.I. Vázquez Vázquez, P. Álvarez-Aránega, Actividad antitumoral de taiwaniaquinoides y compuestos relacionados, (2014). ⟨http://digibug.ugr.es/handle/10481/33608⟩. (Accessed 13 June 2016).

[15] I. Ramírez-Macías, C. Marín, H. Es-Samti, A. Fernández, J.J. Guardia, H. Zentar, A. Agil, R. Chahboun, E. Alvarez-Manzaneda, M. Sánchez-Moreno, Taiwaniaquinoid and abietane quinone derivatives with trypanocidal activity against T. cruzi and Leishmania spp. Parasitol. Int. 61 (2012) 405–413, https://doi.org/10.1016/j.parint.2012.02.001.

[16] S. Tang, Y. Xu, J. He, Y. He, J. Zheng, X. Pan, X. She, Application of a domino Friedel-Crafts acylation/alkylation reaction to the formal syntheses of (+/-)-taiwaniaquinol B and (+/-)-dichroanone, Org. Lett. 10 (2008) 1855–1858, https://doi.org/10.1021/ol800513v.

[17] E. Alvarez-Manzaneda, R. Chahboun, E. Cabrera, E. Alvarez, R. Alvarez-Manzaneda, R. Meneses, H. Es-Samti, A. Fernández, A very efficient route toward the 4a-methyltetrahydrofluorene skeleton: short synthesis of (+/-)-dichroanone and (+/-)-taiwaniaquinone H, J. Org. Chem. 74 (2009) 3384–3388, https://doi.org/10.1021/jo900153y.

[18] G. Majetich, J.M. Shimkus, Concise syntheses of (±)-dichroanone, (±)-dichroanal B, (±)-taiwaniaquinol B, and (±)-taiwaniaquinone D, Tetrahedron Lett. 50 (2009) 3311–3313, https://doi.org/10.1016/j.tetlet.2009.02.074.

[19] J. Deng, R. Li, Y. Luo, J. Li, S. Zhou, Y. Li, J. Hu, A. Li, Divergent total synthesis of taiwaniaquinones A and F and taiwaniaquinols B and D, Org. Lett. 15 (2013) 2022–2025, https://doi.org/10.1021/ol400717h.

[20] J. Wang, J. Wang, C. Li, Y. Meng, J. Wu, C. Song, J. Chang, Synthesis of 5-epi-taiwaniaquinone G, J. Org. Chem. 79 (2014) 6354–6359, https://doi.org/10.1021/jo500931e.

[21] X. Yan, X. Hu, Protecting-group-free synthesis of taiwaniaquinone H using a one-pot thermal ring expansion/4π-electrocyclization strategy, J. Org. Chem. 79 (2014) 5282–5286, https://doi.org/10.1021/jo5008652.

[22] B.N. Kakde, P. Kumari, A. Bisai, Total synthesis of (±)-taiwaniaquinol F and related taiwaniaquinoids, J. Org. Chem. 80 (2015) 9889–9899, https://doi.org/10.1021/acs.joc.5b01345.

[23] R.M. McFadden, B.M. Stoltz, The catalytic enantioselective, protecting group-free total synthesis of (+)-dichroanone, J. Am. Chem. Soc. 128 (2006) 7738–7739, https://doi.org/10.1021/ja061853f.

[24] M. Node, M. Ozeki, L. Planas, M. Nakano, H. Takita, D. Mori, S. Tamatani, T. Kajimoto, Efficient asymmetric synthesis of abeo-abietane-type diterpenoids by using the intramolecular Heck reaction, J. Org. Chem. 75 (2010) 190–196, https://doi.org/10.1021/jo901972b.

[25] X. Liao, L.M. Stanley, J.F. Hartwig, Enantioselective total syntheses of (-)-taiwaniaquinone H and (-)-taiwaniaquinol B by iridium-catalyzed borylation and palladium-catalyzed asymmetric α-arylation, J. Am. Chem. Soc. 133 (2011) 2088–2091, https://doi.org/10.1021/ja110215b.

[26] K. Kikushima, J.C. Holder, M. Gatti, B.M. Stoltz, Palladium-catalyzed asymmetric conjugate addition of arylboronic acids to five-, six-, and seven-membered β-substituted cyclic enones: enantioselective construction of all-carbon quaternary stereocenters, J. Am. Chem. Soc. 133 (2011) 6902–6905, https://doi.org/10.1021/ja200664x.

[27] M. Ozeki, M. Satake, T. Toizume, S. Fukutome, K. Arimitsu, S. Hosoi, T. Kajimoto, H. Iwasaki, N. Kojima, M. Node, M. Yamashita, First asymmetric total synthesis of (+)-taiwaniaquinol D and (−)-taiwaniaquinone D by using intramolecular Heck reaction, Tetrahedron 69 (2013) 3841–3846, https://doi.org/10.1016/j.tet.2013.03.051.

[28] S.E. Shockley, J.C. Holder, B.M. Stoltz, A catalytic, enantioselective formal synthesis of (+)-dichroanone and (+)-taiwaniaquinone H, Org. Lett. 16 (2014) 6362–6365, https://doi.org/10.1021/ol5031537.

[29] E. Alvarez-Manzaneda, R. Chahboun, E. Cabrera, E. Alvarez, A. Haidour, J. M. Ramos, R. Alvarez-Manzaneda, M. Hmamouchi, H. Es-Samti, A thermal 6pi electrocyclization strategy towards taiwaniaquinoids. First enantiospecific synthesis of (-)-taiwaniaquinone G, Chem. Commun.. (2009) 592–594, https://doi.org/10.1039/b816812a.

[30] E. Alvarez-Manzaneda, R. Chahboun, E. Cabrera, E. Alvarez, A. Haidour, J. M. Ramos, R. Alvarez-Manzaneda, Y. Charrah, H. Es-Samti, An enantiospecific route towards taiwaniaquinoids. First synthesis of (-)-taiwaniaquinone H and (-)-dichroanone, Org. Biomol. Chem. 7 (2009) 5146–5155, https://doi.org/10.1039/b916209g.

[31] C.K. Jana, R. Scopelliti, K. Gademann, A synthetic entry into the taiwaniaquinoids based on a biogenetic hypothesis: total synthesis of (-)-taiwaniaquinone H, Chemistry 16 (2010) 7692–7695, https://doi.org/10.1002/chem.201001085.

[32] E. Alvarez-Manzaneda, R. Chahboun, E. Alvarez, R. Tapia, R. Alvarez-Manzaneda, Enantioselective total synthesis of cytotoxic taiwaniaquinones A and F, Chem. Commun. 46 (2010) 9244–9246, https://doi.org/10.1039/c0cc03763j.

[33] R. Tapia, J.J. Guardia, E. Alvarez, A. Haidour, J.M. Ramos, R. Alvarez-Manzaneda, R. Chahboun, E. Alvarez-Manzaneda, General access to taiwaniaquinoids based on a hypothetical abietane C7-C8 cleavage biogenetic pathway, J. Org. Chem. 77 (2012) 573–584, https://doi.org/10.1021/jo202163y.

[34] Q. Yuan, Z. Liu, C. Xiong, L. Wu, J. Wang, J. Ruan, A novel, broad-spectrum antitumor compound containing the 1-hydroxycyclohexa-2,5-dien-4-one group: The disclosure of a new antitumor pharmacophore in protoapigenone 1, Bioorg. Med. Chem. Lett. 21 (2011) 3427–3430, https://doi.org/10.1016/j.bmcl.2011.03.108.

[35] A.A. Vieira, I.R. Brandão, W.O. Valença, C.A. de Simone, B.C. Cavalcanti, C. Pessoa, T.R. Carneiro, A.L. Braga, E.N. da Silva, Hybrid compounds with two redox centres: modular synthesis of chalcogen-containing lapachones and studies on their antitumor activity, Eur. J. Med Chem. 101 (2015) 254–265, https://doi.org/10.1016/j.ejmech.2015.06.044.

[36] N. Bouchmaa, M. Tilaoui, Y. Boukharsa, A. Jaâfari, H.A. Mouse, My Ali Oukerrou, J. Taoufik, M. Ansar, A. Zyad, In vitro antitumor activity of newly synthesized pyridazin-3(2H)-one derivatives via apoptosis induction, Pharm. Chem. J. 51 (2018) 893–901, https://doi.org/10.1007/s11094-018-1712-x.

[37] C.R. Kleiveland, Peripheral blood mononuclear cells, in: K. Verhoeckx, P. Cotter, I. López-Expósito, C. Kleiveland, T. Lea, A. Mackie, T. Requena, D. Swiatecka, H. Wichers (Eds.), The Impact of Food Bioactives on Health: in Vitro and Ex Vivo Models, Springer, Cham (CH), 2015. ⟨http://www.ncbi.nlm.nih.gov/books/NBK500157/⟩. accessed September 9, 2020.

[38] J. Drost, R.H. van Jaarsveld, B. Ponsioen, C. Zimberlin, R. van Boxtel, A. Buijs, N. Sachs, R.M. Overmeer, G.J. Offerhaus, H. Begthel, J. Korving, M. van de Wetering, G. Schwank, M. Logtenberg, E. Cuppen, H.J. Snippert, J.P. Medema, G.J. P.L. Kops, H. Clevers, Sequential cancer mutations in cultured human intestinal stem cells, Nature 521 (2015) 43–47, https://doi.org/10.1038/nature14415.

[39] F. Hecht, C.F. Pessoa, L.B. Gentile, D. Rosenthal, D.P. Carvalho, R.S. Fortunato, The role of oxidative stress on breast cancer development and therapy, Tumour Biol. 37 (2016) 4281–4291, https://doi.org/10.1007/s13277-016-4873-9.

[40] R.K. Blackman, K. Cheung-Ong, M. Gebbia, D.A. Proia, S. He, J. Kepros, A. Jonneaux, P. Marchetti, J. Kluza, P.E. Rao, Y. Wada, G. Giaever, C. Nislow, Mitochondrial electron transport is the cellular target of the oncology drug elesclomol, PLoS One 7 (2012), e29798, https://doi.org/10.1371/journal.pone.0029798.

[41] M.-L. Hu, Dietary polyphenols as antioxidants and anticancer agents: more questions than answers, Chang Gung Med J. 34 (2011) 449–460.

[42] J. Bouayed, T. Bohn, Exogenous antioxidants–double-edged swords in cellular redox state: Health beneficial effects at physiologic doses versus deleterious effects at high doses, Oxid. Med. Cell. Longev. 3 (2010) 228–237, https://doi.org/10.4161/oxim.3.4.12858.

[43] N. Mut-Salud, P.J. Álvarez, J.M. Garrido, E. Carrasco, A. Aránega, F. Rodríguez-Serrano, Antioxidant INtake and Antitumor Therapy: toward Nutritional Recommendations for Optimal Results, Oxid. Med. Cell. Longev. 2016 (2016) 6719534, https://doi.org/10.1155/2016/6719534.

[44] S. Saeidnia, M. Abdollahi, Antioxidants: friends or foe in prevention or treatment of cancer: the debate of the century, Toxicol. Appl. Pharmacol. 271 (2013) 49–63, https://doi.org/10.1016/j.taap.2013.05.004.

[45] L. Tong, C.-C. Chuang, S. Wu, L. Zuo, Reactive oxygen species in redox cancer therapy, Cancer Lett. 367 (2015) 18–25, https://doi.org/10.1016/j.canlet.2015.07.008.

[46] P. Poprac, K. Jomova, M. Simunkova, V. Kollar, C.J. Rhodes, M. Valko, Targeting free radicals in oxidative stress-related human diseases, Trends Pharmacol. Sci. 38 (2017) 592–607, https://doi.org/10.1016/j.tips.2017.04.005.

[47] G.V. Martins, A.P.M. Tavares, E. Fortunato, M.G.F. Sales, Paper-based sensing device for electrochemical detection of oxidative stress biomarker 8-hydroxy-2′-deoxyguanosine (8-OHdG) in point-of-care, Sci. Rep. 7 (2017) 1–10, https://doi.org/10.1038/s41598-017-14878-9.

[48] S. Yu, H.-M. Sheu, C.-H. Lee, Solanum incanum extract (SR-T100) induces melanoma cell apoptosis and inhibits established lung metastasis, Oncotarget 8 (2017) 103509–103517, https://doi.org/10.18632/oncotarget.21508.
[49] G. Mariño, M. Niso-Santano, E.H. Baehrecke, G. Kroemer, Self-consumption: the interplay of autophagy and apoptosis, Nat. Rev. Mol. Cell Biol. 15 (2014) 81–94, https://doi.org/10.1038/nrm3735.
[50] M. Sorice, Crosstalk of autophagy and apoptosis, Cells 11 (2022) 1479, https://doi.org/10.3390/cells11091479.
[51] J. Yu, C. Chen, T. Xu, M. Yan, B. Xue, Y. Wang, C. Liu, T. Zhong, Z. Wang, X. Meng, D. Hu, X. Yu, Pseudolaric acid B activates autophagy in MCF-7 human breast cancer cells to prevent cell death, Oncol. Lett. 11 (2016) 1731–1737, https://doi.org/10.3892/ol.2016.4103.
[52] S. Srivastava, R.R. Somasagara, M. Hegde, M. Nishana, S.K. Tadi, M. Srivastava, B. Choudhary, S.C. Raghavan, Quercetin, a Natural Flavonoid interacts with DNA, arrests cell cycle and causes tumor regression by activating mitochondrial pathway of apoptosis, Sci. Rep. 6 (2016), https://doi.org/10.1038/srep24049.
[53] S.H. van Rijt, I. Romero-Canelón, Y. Fu, S.D. Shnyder, P.J. Sadler, Potent organometallic osmium compounds induce mitochondria-mediated apoptosis and S-phase cell cycle arrest in A549 non-small cell lung cancer cells, Metallomics 6 (2014) 1014–1022, https://doi.org/10.1039/c4mt00034j.
[54] P. Chu, G. Han, A. Ahsan, Z. Sun, S. Liu, Z. Zhang, B. Sun, Y. Song, Y. Lin, J. Peng, Z. Tang, Phosphocreatine protects endothelial cells from Methylglyoxal induced oxidative stress and apoptosis via the regulation of PI3K/Akt/eNOS and NF-κB pathway, Vasc. Pharmacol. 91 (2017) 26–35, https://doi.org/10.1016/j.vph.2016.08.012.
[55] S. Xu, H. Yao, S. Luo, Y.-K. Zhang, D.-H. Yang, D. Li, G. Wang, M. Hu, Y. Qiu, X. Wu, H. Yao, W. Xie, Z.-S. Chen, J. Xu, A novel potent anticancer compound Optimized from a natural oridonin scaffold induces apoptosis and cell cycle arrest through the mitochondrial pathway, J. Med. Chem. 60 (2017) 1449–1468, https://doi.org/10.1021/acs.jmedchem.6b01652.
[56] G.-S. Wu, J.-J. Lu, J.-J. Guo, Y.-B. Li, W. Tan, Y.-Y. Dang, Z.-F. Zhong, Z.-T. Xu, X.-P. Chen, Y.-T. Wang, Ganoderic acid DM, a natural triterpenoid, induces DNA damage, G1 cell cycle arrest and apoptosis in human breast cancer cells, Fitoterapia 83 (2012) 408–414, https://doi.org/10.1016/j.fitote.2011.12.004.
[57] D. Reddy, R. Kumavath, P. Ghosh, D. Barh, Lanatoside C induces G2/M cell cycle arrest and suppresses cancer cell growth by attenuating MAPK, Wnt, JAK-STAT, and PI3K/AKT/mTOR signaling pathways, Biomolecules 9 (2019) 792, https://doi.org/10.3390/biom9120792.
[58] S. Zhao, Y. Tang, R. Wang, M. Najafi, Mechanisms of cancer cell death induction by paclitaxel: an updated review, Apoptosis 27 (2022) 647–667, https://doi.org/10.1007/s10495-022-01750-z.
[59] Q. Chen, J. Kang, C. Fu, The independence of and associations among apoptosis, autophagy, and necrosis, Signal. Transduct. Target. Ther. 3 (2018) 18, https://doi.org/10.1038/s41392-018-0018-5.
[60] O. Morana, W. Wood, C.D. Gregory, The apoptosis paradox in cancer, Int. J. Mol. Sci. 23 (2022) 1328, https://doi.org/10.3390/ijms23031328.
[61] S. Sajadimajd, M. Khazaei, Oxidative stress and cancer: the role of Nrf2, Curr. Cancer Drug Targets 18 (2018) 538–557, https://doi.org/10.2174/1568009617666171002144228.
[62] J.D. Hayes, A.T. Dinkova-Kostova, K.D. Tew, Oxidative stress in cancer, Cancer Cell 38 (2020) 167–197, https://doi.org/10.1016/j.ccell.2020.06.001.
[63] J. Shin, M.-H. Song, J.-W. Oh, Y.-S. Keum, R.K. Saini, Pro-oxidant actions of carotenoids in triggering apoptosis of cancer cells: a review of emerging evidence, Antioxidants 9 (2020), https://doi.org/10.3390/antiox9060532.
[64] S. Shalini, L. Dorstyn, S. Dawar, S. Kumar, Old, new and emerging functions of caspases, Cell Death Differ. 22 (2015) 526–539, https://doi.org/10.1038/cdd.2014.216.
[65] J.G. Nirmala, M. Lopus, Cell death mechanisms in eukaryotes, Cell Biol. Toxicol. 36 (2020) 145–164, https://doi.org/10.1007/s10565-019-09496-2.
[66] E. Carrasco, P.J. Álvarez, C. Melguizo, J. Prados, E. Álvarez-Manzaneda, R. Chahboun, I. Messouri, M.I. Vázquez-Vázquez, A. Aránega, F. Rodríguez-Serrano, Novel merosesquiterpene exerts a potent antitumor activity against breast cancer cells in vitro and in vivo, Eur. J. Med. Chem. 79 (2014) 1–12, https://doi.org/10.1016/j.ejmech.2014.03.071.
[67] K.K. Kaminska, H.C. Bertrand, H. Tajima, W.C. Stafford, Q. Cheng, W. Chen, G. Wells, E.S.J. Arner, E.-H. Chew, Indolin-2-one compounds targeting thioredoxin reductase as potential anticancer drug leads, Oncotarget 7 (2016) 40233–40251, https://doi.org/10.18632/oncotarget.9579.
[68] P. Morales, D. Vara, M. Goméz-Cañas, M.C. Zúñiga, C. Olea-Azar, P. Goya, J. Fernández-Ruiz, I. Díaz-Laviada, N. Jagerovic, Synthetic cannabinoid quinones: preparation, in vitro antiproliferative effects and in vivo prostate antitumor activity, Eur. J. Med. Chem. 70 (2013) 111–119, https://doi.org/10.1016/j.ejmech.2013.09.043.
[69] H. Raza, A. John, J. Shafarin, Potentiation of LPS-induced apoptotic cell death in human hepatoma HepG2 cells by aspirin via ROS and Mitochondrial dysfunction: protection by N-acetyl cysteine, PLoS One 11 (2016), e0159750, https://doi.org/10.1371/journal.pone.0159750.
[70] H. Xia, K.W. Lee, J. Chen, S.N. Kong, K. Sekar, A. Deivasigamani, V. P. Seshachalam, B.K.P. Goh, L.L. Ooi, K.M. Hui, Simultaneous silencing of ACSL4 and induction of GADD45B in hepatocellular carcinoma cells amplifies the synergistic therapeutic effect of aspirin and sorafenib, Cell Death Discov. 3 (2017) 17058, https://doi.org/10.1038/cddiscovery.2017.58.
[71] L. Singh, N. Pushker, N. Saini, S. Sen, A. Sharma, S. Bakhshi, B. Chawla, S. Kashyap, Expression of pro-apoptotic Bax and anti-apoptotic Bcl-2 proteins in human retinoblastoma, Clin. Exp. Ophthalmol. 43 (2015) 259–267, https://doi.org/10.1111/ceo.12397.
[72] G.H. Hwang, Y.J. Jeon, H.J. Han, S.H. Park, K.M. Baek, W. Chang, J.S. Kim, L. K. Kim, Y.-M. Lee, S. Lee, J.-S. Bae, J.-G. Jee, M.Y. Lee, Protective effect of butylated hydroxylanisole against hydrogen peroxide-induced apoptosis in primary cultured mouse hepatocytes, J. Vet. Sci. 16 (2015) 17–23, https://doi.org/10.4142/jvs.2015.16.1.17.
[73] S. Nagata, Apoptosis and clearance of apoptotic cells, Annu. Rev. Immunol. 36 (2018) 489–517, https://doi.org/10.1146/annurev-immunol-042617-053010.
[74] N. Van Opdenbosch, M. Lamkanfi, Caspases in cell death, inflammation, and disease, Immunity 50 (2019) 1352–1364, https://doi.org/10.1016/j.immuni.2019.05.020.
[75] E. Devarajan, A.A. Sahin, J.S. Chen, R.R. Krishnamurthy, N. Aggarwal, A.-M. Brun, A. Sapino, F. Zhang, D. Sharma, X.-H. Yang, A.D. Tora, K. Mehta, Down-regulation of caspase 3 in breast cancer: a possible mechanism for chemoresistance, Oncogene 21 (2002) 8843.
[76] P.P. Banerjee, A. Bandyopadhyay, S.N. Harsha, R.S. Policegoudra, S. Bhattacharya, N. Karak, A. Chattopadhyay, Mentha arvensis (Linn.)-mediated green silver nanoparticles trigger caspase 9-dependent cell death in MCF7 and MDA-MB-231 cells, Breast Cancer 9 (2017) 265–278, https://doi.org/10.2147/BCTT.S130952.
[77] W. Li, J. Wang, H. Hu, Q. Li, Y. Liu, K. Wang, Functional polysaccharide Lentinan suppresses human breast cancer growth via inducing autophagy and caspase-7-mediated apoptosis, J. Funct. Foods 45 (2018) 75–85, https://doi.org/10.1016/j.jff.2018.03.024.
[78] C.-T. Chang, M. Korivi, H.-C. Huang, V. Thiyagarajan, K.-Y. Lin, P.-J. Huang, J.-Y. Liu, Y.-C. Hseu, H.-L. Yang, Inhibition of ROS production, autophagy or apoptosis signaling reversed the anticancer properties of Antrodia salmonea in triple-negative breast cancer (MDA-MB-231) cells, Food Chem. Toxicol. 103 (2017) 1–17, https://doi.org/10.1016/j.fct.2017.02.019.
[79] X. Wang, S. Wei, Y. Zhao, C. Shi, P. Liu, C. Zhang, Y. Lei, B. Zhang, B. Bai, Y. Huang, H. Zhang, Anti-proliferation of breast cancer cells with itraconazole: hedgehog pathway inhibition induces apoptosis and autophagic cell death, Cancer Lett. 385 (2017) 128–136, https://doi.org/10.1016/j.canlet.2016.10.034.
[80] R. Venkatadri, T. Muni, A.K.V. Iyer, J.S. Yakisich, N. Azad, Role of apoptosis-related miRNAs in resveratrol-induced breast cancer cell death, Cell Death Dis. 7 (2016), e2104, https://doi.org/10.1038/cddis.2016.6.
[81] Y. Choi, M.A. Abdelmegeed, B.-J. Song, Diet high in fructose promotes liver steatosis and hepatocyte apoptosis in C57BL/6J female mice: role of disturbed lipid homeostasis and increased oxidative stress, Food Chem. Toxicol. 103 (2017) 111–121, https://doi.org/10.1016/j.fct.2017.02.039.
[82] L. Yu, X. Liu, Z. Yuan, X. Li, H. Yang, Z. Yuan, L. Sun, L. Zhang, Z. Jiang, SRT1720 alleviates ANIT-induced cholestasis in a Mouse Model, Front. Pharmacol. 8 (2017) 256, https://doi.org/10.3389/fphar.2017.00256.
[83] A.R.H. da Silva, L. da, R. Moreira, E. da, S. Brum, M.L. de Freitas, A.A. Boligon, M. L. Athayde, S.S. Roman, C.M. Mazzanti, R. Brandão, Biochemical and hematological effects of acute and sub-acute administration to ethyl acetate fraction from the stem bark Scutia buxifolia Reissek in mice, J. Ethnopharmacol. 153 (2014) 908–916, https://doi.org/10.1016/j.jep.2014.03.063.
[84] E. Young, L. Miele, K.B. Tucker, M. Huang, J. Wells, J.-W. Gu, SU11248, a selective tyrosine kinases inhibitor suppresses breast tumor angiogenesis and growth via targeting both tumor vasculature and breast cancer cells, Cancer Biol. Ther. 10 (2010) 703–711, https://doi.org/10.4161/cbt.10.7.12904.